THE DIFFUSION OF OXYGEN, CARBON DIOXIDE, AND INERT GAS IN FLOWING BLOOD

E. E. SPAETH *and* S. K. FRIEDLANDER

From the W. M. Keck Engineering Laboratories, California Institute of Technology, Pasadena, California 91109

ABSTRACT Measurements were made of exchange rates of oxygen, carbon dioxide, and krypton-85 with blood at 37.5°C. Gas transfer took place across a 1 mil silicone rubber membrane. The blood was in a rotating disk boundary layer flow, and the controlling resistance to transfer was the concentration boundary layer. Measured rates were compared with rates predicted from the equation of convective diffusion using velocities derived from the Navier-Stokes equations and diffusivities calculated from the theory for conduction in a heterogeneous medium. The measured absorption rate of krypton-85 was closely predicted by this model. Significant deposition of material onto the membrane surface, resulting in an increased transfer resistance, occurred in one experiment with blood previously used in a nonmembrane type artificial lung. The desorption rate of oxygen from blood at low P_{O_2}[1] was up to four times the corresponding transfer rate of inert gas. This effect is described somewhat conservatively by a local equilibrium form of the convective diffusion equation. The carbon dioxide transfer rate in blood near venous conditions was about twice that of inert gas, a rate significantly greater than predicted by the local equilibrium theory. It should be possible to apply these theoretical methods to predict exchange rates with blood flowing in systems of other geometries.

INTRODUCTION

The use of extracorporeal circulation to restore venous blood to arterial conditions during heart-lung bypass is an established practice today, although less than two decades have elapsed since this procedure was first applied to human patients. The most widely used types of gas exchange devices, or "artificial lungs," contact the blood directly with the gas phase. Although this procedure is highly efficient with respect to gas exchange, it has been found to cause toxic degradation of the blood (4, 16), resulting in an unusually high mortality rate. Prolonged use of such a lung is therefore prohibited.

[1] For abbreviations used see Nomenclature at end of text.

In order to significantly reduce the amount of blood damage, it is necessary to employ a method similar to that used in living organisms—namely, the introduction of a thin, semipermeable membrane between the blood and gas phases. Associated with the use of a membrane, however, is the additional resistance to mass transfer of both the membrane and the slowly moving blood adjacent to it. For silicone rubber membranes, most of the transfer resistance is due to the blood itself and not the membrane, so in the design of this type of artificial lung one must be able to estimate mass transfer rates in flowing blood.

This paper reports the results of a study of convective diffusion in blood in a system with characteristic dimensions much greater than the size of the red cell. In this case it is reasonable to treat the blood as a homogeneous fluid, using the normal transport equations as the basis of a general theory. Such a theory could not be expected to apply to the processes occurring in the capillaries, where the scale of the system is similar to the red cell diameter, but could be expected to apply to processes occurring in extracorporeal devices and the larger blood vessels. In the case of exchange in the capillaries, this theory would present a limiting case, similar to the use of continuum fluid mechanics to describe blood flow through the capillaries.

ANALYTICAL CONSIDERATIONS

The general equation for the convective diffusion of a species i in a homogeneous, incompressible fluid can be written (17, 3):

$$\underbrace{\frac{D}{Dt}(n_i)}_{\substack{\text{Rate of change in a} \\ \text{flowing element}}} = \underbrace{-\nabla\cdot\mathbf{J}_i}_{\substack{\text{Net diffusion from} \\ \text{the element}}} + \underbrace{R_i}_{\substack{\text{Net chemical reaction} \\ \text{in the element}}} \tag{1}$$

where D/Dt ( ) is the substantial derivative $\partial/\partial t$ ( ) + $\mathbf{v}\cdot\nabla$ ( ). Consider the special set of species, n_{ik}, $k = 1, \cdots, r$, where n_{i1} refers to the concentration of the unreacted form of molecular species i, and $n_{i2}, \cdots, n_{ir}$ refer to the concentration of i present in the various forms resulting from chemical reactions with other dissolved species in the fluid. For example, in the case of oxygen and blood n_{O_21} refers to the concentration of physically dissolved oxygen and $n_{O_22}, \cdots, n_{O_2r}$ refer to the concentration of oxygen present in the various forms of oxyhemoglobin. If the convective diffusion equations for n_{ik} are summed over the set $k = 1, \cdots, r$, the resulting equation is a mass balance on species i, including all of its chemically reacted forms. Since the total mass of species i is not changed by the chemical reactions, the sum of the reaction terms must vanish. The resulting equation is then:

$$\frac{D}{Dt}(n_T)_i = -\nabla\cdot(\mathbf{J}_T)_i \tag{2}$$

where

$$(n_T)_i = n_{i1} + N_i \tag{3}$$

$$N_i = \sum_{k=2}^{r} n_{ik} \tag{4}$$

and

$$(\mathbf{J}_T)_i = \mathbf{J}_{i1} + \sum_{k=2}^{r} \mathbf{J}_{ik} \tag{5}$$

In the physiological literature it is customary to write n_{i1} as the product of a solubility coefficient, α_i, and the partial pressure, or "tension," P_i, of the dissolved species.

The values of N_i corresponding to chemical equilibrium, N_i^*, are generally reported in the literature as a function of P_i, and rearranging equation (2) in terms of this equilibrium value:

$$\underbrace{\frac{D}{Dt}(\alpha_i P_i + N_i^*)}_{\substack{\text{Rate of change of } (n_T)_i \text{ assuming chemical equilibrium in the element}}} = \underbrace{-\nabla\cdot(\mathbf{J}_T)_i}_{\text{Net diffusion to the element}} + \underbrace{\frac{D}{Dt}(N_i^* - N_i)}_{\substack{\text{Rate of change of displacement from chemical equilibrium in the element}}} \tag{6}$$

Equation (6) is a general equation which can be used to describe the transfer of gas in blood flowing as a homogeneous fluid. To solve this equation the following parameters must be specified: (*a*) the velocity field $\mathbf{v}$, (*b*) the solubility α_i, (*c*) the equilibrium relationship $N_i^*(P_i)$, (*d*) the diffusional flux $(\mathbf{J}_T)_i$, and (*e*) the displacement from chemical equilibrium $(N_i^* - N_i)$.

The rheological properties of blood have been studied in detail using coaxial cylinder and capillary viscometers. Since these viscometers are large-scale devices, the measurements can be applied to a homogeneous fluid theory. The viscosity of blood has been found to be non-Newtonian at very low shear rates (19, 20), presumably due to the breakup of red cell clusters. In a strongly sheared system (shear rate > 100 sec^{-1}) the viscosity of blood approaches a constant, "Newtonian" value. Plasma always exhibits Newtonian behavior.

The specification of the velocity field $\mathbf{v}$ is simplified considerably if the non-Newtonian behavior of the blood is neglected. This approximation is probably most acceptable when used to calculate diffusion rates in a fluid flowing past a membrane surface. Mass transfer rates in such systems are generally controlled by the velocity near the surface, and in this region the shear is greatest and the non-Newtonian effects least important.

The solubilities and equilibrium relationships for most of the gases of physiological

interest are available in the literature (9). Less is known about diffusion through blood. Since blood is a highly heterogeneous fluid, the simple Fick's law relationship employing molecular diffusivities cannot be used directly. The usual procedure is to introduce an effective diffusivity which, for the case of dissolved gases diffusing through blood, is defined by:

$$\mathbf{J}_{i,B} = -D_{i,B}\alpha_i \nabla P_i \tag{7}$$

The effective diffusivity is a function of both the volume fraction of suspended phase (or hematocrit value) and the relative permeability of the suspended phase to that of the continuous phase, as well as a function of temperature and viscosity.

TABLE I

THE DIFFUSIVITY OF OXYGEN IN WATER, PLASMA, AND CONCENTRATED HEMOGLOBIN SOLUTION

	D_{O_2,H_2O} (cm²/sec)		$D_{O_2,P}$ (cm²/sec)		$D_{O_2,35\%Hb}$	$D_{O_2,35\%Hb}$
Experimenter	25°C	37.5°C	25°C	37.5°C	25°C	$D_{O_2,P}$
Yoshida et al (29)	—	2.76 $\times 10^{-5}$	§1.24 $\times 10^{-5}$	§1.66 $\times 10^{-5}$	—	—
Goldstick (6)	2.13 $\times 10^{-5}$	*2.89 $\times 10^{-5}$	‡1.21 $\times 10^{-5}$	‡1.63 $\times 10^{-5}$	0.73 $\times 10^{-5}$	0.60
Keller and Friedlander (12)	2.05 $\times 10^{-5}$	*2.66 $\times 10^{-5}$	‡1.17 $\times 10^{-5}$	‡1.57 $\times 10^{-5}$	0.75 $\times 10^{-5}$	0.64

* Stokes-Einstein correction of value measured at 25°C.
‡ Stokes-Einstein correction of D_{O_2,H_2O}.
§ Stokes-Einstein correction of $D_{O_2,s}$

Effective diffusivities can be calculated using equations based on Maxwell's treatment of conduction in a suspension of noninteracting particles (2). The equations given by Fricke (5) for a suspension of oblate spheroids were used in this study, along with his empirically determined shape factor. The diffusivities of oxygen in plasma and concentrated oxyhemoglobin solution (assumed equivalent to the red cell interior) are listed in Table I. The transfer resistance of the red cell membrane was neglected. The effective diffusivity of oxygen through blood, determined in this way, was then corrected using the Stokes-Einstein theory of diffusion to obtain the effective diffusivities of krypton and carbon dioxide in blood.

Since the diffusion of oxygen through unsaturated hemoglobin solutions is known to be facilitated by the simultaneous diffusion of oxyhemoglobin, the effective diffusivity of oxygen through unsaturated blood might be expected to depend on the oxygen partial pressure. Considerable controversy exists as to the importance of this effect in blood. Recent measurements of the diffusion of hemoglobin molecules

in hemoglobin solutions at concentrations comparable to the red cell interior show a dramatic fall in diffusivity with increasing concentration (21). The effect may be even more severe in intact red cells if internal structure exists. The importance of the facilitation theory in describing oxygen diffusion through intact red cells is also questionable on the basis of the theoretical analysis of Keller and Friedlander (12), which shows that the near-equilibrium behavior necessary for facilitation to occur might not be established in hemoglobin layers on the order of the thickness of the red cell. Both the inert and the facilitated effective oxygen diffusivities in blood are compared with the experimental results to be presented here.

The last term on the right in equation (6) describes the departure of the system from local chemical equilibrium. The importance of this term can be estimated using measurements of the equilibration rates of red cells (25, 15, 9) since the changes in oxygen and carbon dioxide content occur primarily within the cells. It is important to determine this displacement from chemical equilibrium locally in the flow field since the velocity of the red cells, and therefore their effective residence time as they travel through the concentration gradient, varies with position.

It is interesting to consider several other studies concerning gas transport in blood, from the point of view of equation (6). Marx et al. (18) studied the non-convective, unsteady-state oxygen uptake rate of a horizontal blood film separated from a flowing gas stream by a silicone rubber membrane. They simplified equation (6) by assuming local chemical equilibrium ($N_{O_2} = N^*_{O_2}$) and a constant value for $D_{O_2,B}$:

$$\frac{\partial}{\partial t}(\alpha_{O_2} P_{O_2} + N^*_{O_2}) = D_{O_2,B}\,\alpha_{O_2} \nabla^2 P_{O_2} \tag{8}$$

Since oxygen was diffusing from a pure gas stream into the blood, the diffusion occurred mostly through saturated blood, with the unsaturated region confined to a thin "advancing front." The experimental value obtained for $D_{O_2,B}$ should thus be close to the effective diffusivity of oxygen in saturated blood. The times required for the experimental measurements ranged from less than 1 min to more than 20 min, long enough for significant red cell sedimentation to occur, but this effect was neglected in their analysis. Since the gas stream was below the blood layer, settling of the red cells would tend to shorten the diffusion path, resulting in a high value for the measured diffusivity. Additional measurements of this diffusivity would be desirable.

Landino et al. (14) discuss transfer to flowing blood employing the same assumptions as Marx et al., but do not provide experimental verification of their results. Buckles (1) has recently completed a study on steady-state oxygen transfer to blood flowing through a hollow silicone rubber fiber. The theoretical analysis employed in this work also assumes local chemical equilibrium and constant $D_{O_2,B}$, and uses the velocity profile predicted by integration of the Casson equation (20) to account for

non-Newtonian effects. The appropriate form of equation (6), neglecting axial diffusion, is:

$$v(r)\frac{\partial}{\partial z}\left[\alpha_{O_2}P_{O_2} + N^*_{O_2}\right] = D_{O_2,B}\alpha_{O_2}\left[\frac{1}{r}\frac{\partial}{\partial r}\left(r\frac{\partial P_{O_2}}{\partial r}\right)\right] \tag{9}$$

The theory was tested with some success in a few experiments with blood, during which oxygen was transferred from a gas stream (P_{O_2} = 686 mm Hg, P_{CO_2} = 36 mm Hg) to reduced blood (P_{O_2} = 0 mm Hg, P_{CO_2} = 36 mm Hg).

Weissman and Mockros (28) reported the preliminary findings of a similar study on oxygen transfer to blood initially 75% saturated, flowing through a silicone rubber fiber. They assume local chemical equilibrium, constant $D_{O_2,B}$, and Poiseuille flow, and neglect the transfer resistance of the tube wall. They found that this model could be fitted to the experimental data over a range of flow rates and tube sizes, by properly selecting the value of $D_{O_2,B}$.

A problem in interpreting experimental results from the fiber system is that the measurement obtained represents the transfer rate integrated over the length of the tube. Deviations in the local transfer rate with axial position are difficult to detect, since they are averaged into the measured integral rate. In our study, which was initiated independently of the fiber studies mentioned above, this problem was avoided by using a one-dimensional mass transfer system. Flow through a hollow tube is an example of the class of internal flows termed "parallel flow" (i.e. there is only one velocity component), while the system used in the work presented here involves an external "boundary layer flow," which is multidimensional. Since there are advantages associated with each type of flow, it is important to study the behavior of both.

EXPERIMENTAL APPARATUS AND PROCEDURES

Apparatus

The experimental system used to test the applicability of equation (6) to gas transfer in blood was a new version of the rotating disk system (17). Two important features of the rotating disk system are (*a*) the equations describing the transfer of inert material have exact, steady-state solutions, and (*b*) the diffusion boundary layer thickness, and therefore the transfer rate to the disk, is not a function of radial position, making the transfer process one-dimensional. This type of one-dimensional mass transfer system is particularly advantageous, since the measured transfer rate then represents a uniform local rate, rather than the integration of a variable local rate over the dimensions of the system.

In our experiments, the surface of the rotating disk was a semipermeable membrane, which introduces an additional mass transfer resistance. It can easily be shown (27) that the solution to equation (6) for the transfer of an inert dissolved gas to a rotating membrane disk is given by:

$$\frac{\Delta P}{J} = [1.61D_{i,f}^{-2/3}\nu^{1/6}\alpha^{-1}]\omega^{-1/2} + \frac{\delta_m}{\Phi_m} \tag{10}$$

where ΔP is the total partial pressure difference across the membrane and fluid boundary layer. For the case of a chemically reacting species this relation does not hold, and it is necessary to solve equation (6) directly.

The rotating disk apparatus used in this study is shown schematically in Fig. 1. The external housing is constructed of Lucite, and all internal surfaces which contact the fluid are Teflon

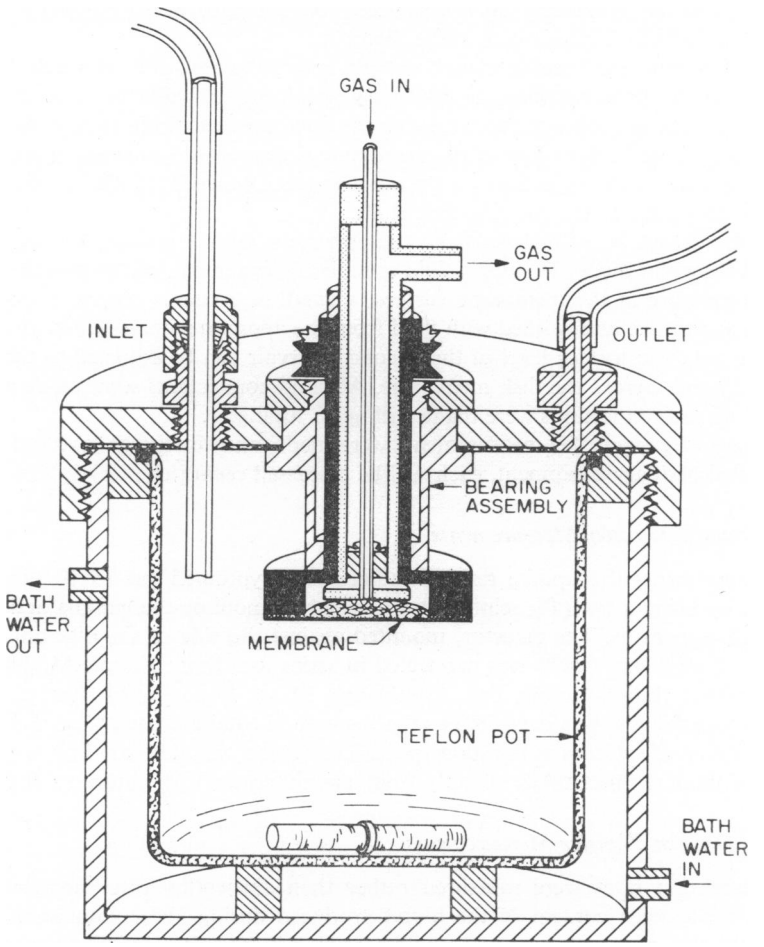

FIGURE 1 A schematic diagram of the rotating disk apparatus.

with the exception of the rotating disk and shaft (stainless steel), and the bearing assembly (nylon). The apparatus is maintained at constant temperature by a circulating water bath. The rotating portion of the apparatus is drawn-in solid in Fig. 1; the remaining pieces of the disk assembly are fixed. The disk is rotated by a geared pulley system driven by a variable speed DC motor. A Teflon-coated magnetic stirrer is placed in the fluid chamber to provide complete mixing when desired.

The surface of the disk is a Dacron-backed silicone rubber membrane [General Electric Co., Schenectady, N. Y. (24)], cemented onto the stainless steel disk body with G.E. RTV

102 cement. This membrane is composed of two 0.5 mil silicone rubber sheets laminated together to eliminate pin holes, and attached on one side to a loosely woven mat of 25 μ Dacron fibers to provide mechanical strength.

The fluid is introduced into the apparatus through the movable Teflon inlet tube. Initially the tube extends to the bottom of the Teflon pot, so that no bubbles will be formed during the filling. When the fluid chamber is nearly filled, the inlet tube is raised above the level of the disk surface, and any remaining gas is displaced from the apparatus by tilting it so that the outlet tube becomes the highest point in the chamber.

During an experimental measurement, wet gas enters the apparatus through the stainless steel inlet tube and flows between the stationary stainless steel baffle and the rotating back-surface of the silicone rubber membrane. The gas flow rate is set high enough to insure that the gas tension at the back-surface of the membrane is that of the gas entering the apparatus. The gas stream leaves the apparatus via the annular space between the inlet tube and the wall of the stationary core of the rotating disk shaft.

Fluid samples can be withdrawn from the apparatus with a syringe, through a syringe stopper not shown in Fig. 1. To supply fluid to replace this sample, and to provide a constant hydrostatic pressure at the membrane surface, a small reservoir is connected to the outlet tube of the apparatus, and is filled with fluid from the apparatus immediately after displacement of the gas. The surface level of this second reservoir can be adjusted to eliminate any pressure difference across the disk membrane. All fluid connections were made with plastic tubing and all gas connections were made with glass tubing.

Three types of gas transfer measurements were made, and since each involved a different assemblage of auxiliary equipment, each will be discussed separately.

Krypton Transfer Measurements

In these experiments the uptake rate of radioactive krypton-85 gas (5–10 mc/liter) was determined by using a NaI(Tl) scintillation detector to monitor the gamma activity of the rotating disk apparatus. The detector, mounted against the side of the disk apparatus and shielded by 2-inch lead bricks was connected in series to a Baird Atomic Model 250 single channel analyzer (Baird-Atomic, Inc., Cambridge, Mass.) and a Baird Atomic Model 132 scaler. The transfer rate was measured as the increase in total activity of the disk apparatus over a fixed time of rotation at constant speed. The system was calibrated by comparing the activities of fluid samples taken directly from the apparatus with saturated fluid samples.

Oxygen Transfer Measurements

Oxygen desorption rates were measured rather than absorption rates because the small changes in the oxygen content of the blood produced during absorption were difficult to measure. The rate of oxygen removal was determined by flushing wet nitrogen gas through the apparatus, stripping oxygen from the fluid, and collecting the resulting trace oxygen gas stream for a fixed period of rotation at constant speed, by displacement of an oxygen free $MnSO_4$ solution. Morgan and Stumm (22) have shown that the oxidation of Mn(II) by dissolved oxygen at 25°C proceeds heterogeneously and autocatalytically, with a reaction rate dependent on the second power of the hydroxide ion concentration. Thus, the reaction can be controlled by varying the pH of the solution; at pH $>$ 10 the reaction proceeds rapidly and at pH $<$ 7 the reaction is effectively frozen. The amount of oxidized manganese formed is directly proportional to the oxygen concentration, and is reproducible at a given pH and temperature. The oxidized manganese can be measured spectrophotometrically, following reaction with *o*-tolidine.

During the collection of the gas sample, the pressure within the rotating disk was maintained at its normal value by setting the flow rate of $MnSO_4$ solution leaving the collection flask equal to the flow rate of the gas leaving the apparatus. Blanks were obtained by shunting the nitrogen gas past the apparatus. A standard curve, obtained by adding aliquots of distilled water of known oxygen content to a series of nitrogen blanks, was linear to within $\pm$ 2% over the range 1–3 μmole total collected oxygen (27). The development time for the *o*-tolidine reaction at room temperature was about 15 min.

Carbon Dioxide Transfer Measurements

The rate of carbon dioxide removal was determined by flushing wet nitrogen gas through the apparatus, stripping carbon dioxide from the fluid, and passing the resulting trace carbon dioxide gas stream though a Beckman L/B Infrared Analyzer (Model 15a) (Beckman Instruments, Inc., Fullerton, Calif.). For a fixed flow rate of gas the concentration of the stream is directly proportional to the transfer rate. This measurement is not a time average, but an instantaneous measurement of the transfer rate, providing a check on the time required to establish steady state. This time was assumed to be negligible in the krypton and oxygen experiments, and indeed, these carbon dioxide measurements showed that the transient behavior of the rotating disk system was limited to less than the first 2% of the time period required to measure an oxygen or krypton transfer rate.

Source and Treatment of the Blood

The blood used during the exploratory phase of this study was obtained from a Los Angeles hospital. It was the residual blood from an artificial lung (nonmembrane type) that had been used in surgery, and was citrated, as well as heparinized. Initial experiments showed that this blood had deteriorated during the course of surgery and in subsequent experiments freshly drawn blood was used. The blood was obtained from the Los Angeles County Blood Bank and contained 0.36% (w/v) sodium citrate. Within several hours of the time it was drawn, the blood was prepared for the experiment by bringing it to body temperature and adjusting it to the desired gas tension by gently bubbling gas through it. Large bubbles ($d > 0.5$ cm) were used to minimize protein denaturation and the formation of residual bubbles. When the blood reached the desired conditions, it was introduced into the rotating disk apparatus as described above. The blood was stirred between experimental measurements to eliminate sedimentation effects. Samples were taken from disk height within the apparatus both before and after the series of measurements, and used to characterize the blood. The total blood hemoglobin and plasma hemoglobin were determined using the cyanmethemoglobin method (7), and the presence of methemoglobin was checked in a separate spectrophotometric analysis (8). The hematocrit values of the blood samples were obtained both by centrifugation in 1 mm capillary tubes and by Coulter counter measurement of the cell concentration. The viscosity of the blood was measured using two Cannon-Fenske glass capillary viscometers. Two viscometers were used to insure that the "near Newtonian" viscosity (high shear) was measured. The wall shear rates in the viscometers were estimated to be 1000 and 500 sec^{-1}. These values correspond to near Newtonian behavior for blood flow in capillary tubes (20), and indeed the two measured values for the viscosity of blood always agreed within experimental error. The average properties of the blood samples taken from the apparatus are listed in Table II. The experimental results for oxygen transfer in different blood samples were adjusted to these "standard" conditions (with pH = 7.4) so that all the data could be presented on the same plot.

The pH, P_{O_2}, and P_{CO_2} of the blood in the apparatus were measured using the Radiometer

Gas Monitor pH A 927 (The London Co., Westlake, Ohio) with thermostated microelectrodes E5021, 5036, and 5046. The oxygen and carbon dioxide electrodes were calibrated with solutions obtained by bubbling calibrated gas mixtures through distilled water in a device maintained at the electrode temperature (37.5°C).

TABLE II

THE AVERAGE PROPERTIES OF THE BLOOD SAMPLES TAKEN FROM THE ROTATING DISK APPARATUS

Property	Average Value
Total hemoglobin	0.136 ± .01 g/ml
Plasma hemoglobin (initial)	0.0003 ± .0001 g/ml
Plasma hemoglobin (final)	0.0013 ± .0004 g/ml
Viscosity	0.030 ± .004 (cm^2/sec)
Hematocrit value	0.41 ± .04
Methemoglobin	0.002 ± .002 g/ml
Temperature	37.5°C

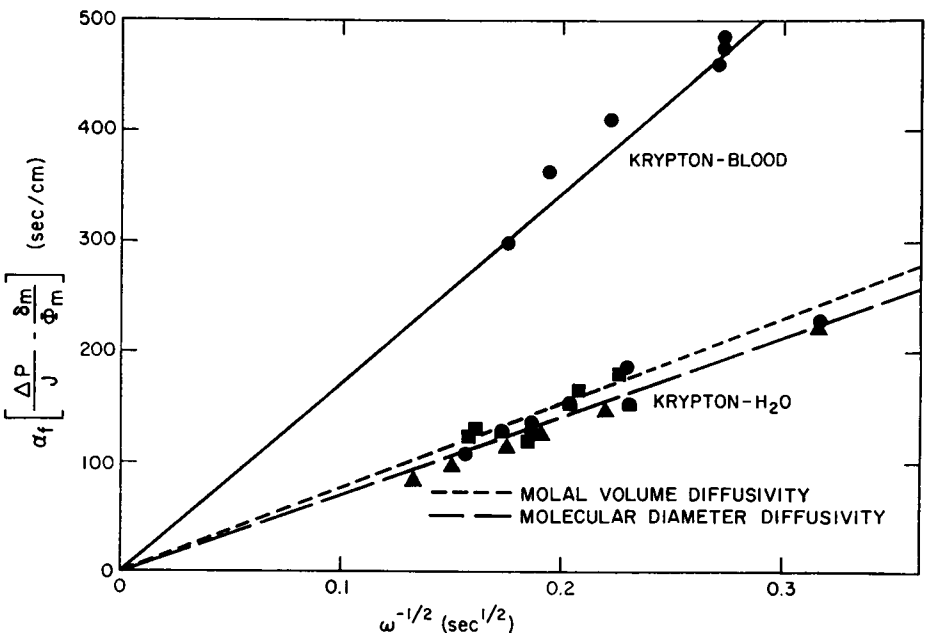

FIGURE 2 A comparison of the experimental data for krypton uptake with the theoretical curves. [α_{Kr,H_2O} = 6.2 × 10^{-6} cc (STP)/cm^3 mm Hg, $\alpha_{Kr,B}$ = 7.25 × 10^{-6} cc (STP)/cm^3 mm Hg, T = 37.5°C].

EXPERIMENTAL RESULTS

Krypton Experiments

The results of the krypton-water experiments are shown in Fig. 2. Each data symbol corresponds to a different membrane, and data points for several of the membranes

include values taken before and after exposure for several hours to freshly drawn blood. No significant increase in membrane resistance occurred during any of the experiments, and the transfer rates are shown to be reproducible from one experiment to another.

Theoretical transfer rates were calculated using the reported solubility (10) of krypton in water. The diffusivity was calculated by correcting the diffusivity of oxygen in water, using both molecular diameter differences obtained from data on properties such as virial coefficients, viscosity, and thermal conductivity, and differences in the molal volumes at the normal boiling point. The ratio of the krypton

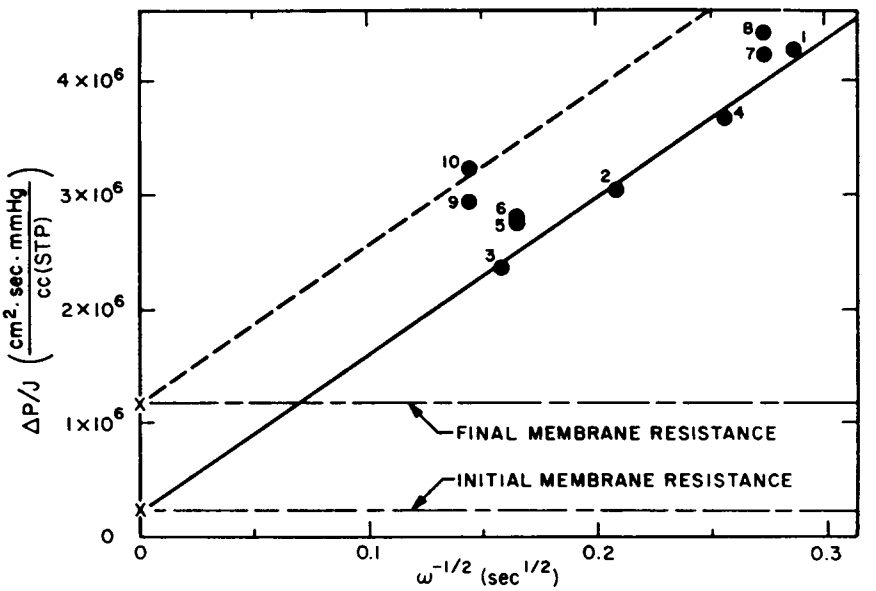

FIGURE 3 A krypton experiment performed with blood previously used in a nonmembrane lung, showing a large increase in membrane resistance with time. The data points are numbered in the order they were taken.

diffusivity to the oxygen diffusivity was found to be 0.94 using an average of the literature values for molecular diameters, and 0.88 using the molal volumes at the normal boiling point. Theoretical lines corresponding to each of these values are drawn on Fig. 2, and both lines are within the experimental error of the data.

The experimental results for krypton transfer to freshly drawn blood are also shown on Fig. 2 along with the theoretical line predicted by equation (10). The viscosity of the blood was measured during the experiment, and the solubility of krypton in blood is reported in the literature (10). The effective diffusivity of krypton in blood was calculated by correcting the effective diffusivity of oxygen, obtained from the Fricke equations. Since theory and experiment agree rather well, it appears that the spinning of the red cells in the shear field does not contribute significantly to transfer over the range of shears covered in these experiments.

Significantly different results were obtained in an early, exploratory krypton experiment with blood taken from a screen-type oxygenator following use in surgery for several hours. This blood had been exposed to the trauma associated with gas-liquid interface oxygenators and with the suction device used to clear the surgical field. Since quantitative characterization of the blood was not made, only qualitative information can be drawn from the results. The data points shown in Fig. 3 are numbered in the order they were taken, each point representing an increase in elapsed time of 10–15 min. The first four points lie on a straight line drawn through the membrane resistance, as theory predicts. Succeeding points then show an ordered increase in total resistance $\Delta P/J$. Following the experiment, the membrane was observed to have a granular, reddish-brown film deposited on it. The membrane was kept submerged in distilled water while the apparatus was cleaned, and an experiment was then performed with krypton and water, using the fouled membrane. Extrapolation of these data for water gave a new, fivefold higher value for the membrane resistance, as shown, and a line originating at this value of the resistance and drawn parallel to the original blood line passes near the final data point. Thus, the observed increase in transfer resistance resulted from the deposit on the membrane. This effect was not observed in experiments with freshly drawn blood. The magnitude of this increase in membrane resistance, and its growth rate indicate that it would limit the useful life of a membrane oxygenator. How important this effect is in the operation of membrane oxygenators is an important unanswered question; this effect would completely change the nature of the transfer process from a boundary layer limited process to a membrane limited one.

Oxygen Experiments

The measured oxygen transfer rate in water at 37.5°C was found to be within experimental error of the theoretical transfer rate, as shown in Fig. 4. The data include values taken before and after use of the membrane in fresh blood experiments. Again, the membrane permeabilities and transfer rates are reproducible to within a few per cent of theoretical behavior, so no significant, ordered change in the permeability of silicone rubber membranes to oxygen occurs during exposure of the membranes to fresh blood for periods up to 4 hr.

The transfer rates measured during the deoxygenation of several blood samples at various oxygen pressures are presented in Table III and Fig. 5. During these experiments there was a simultaneous desorption of carbon dioxide. The data fall near the theoretical line for oxygen diffusion through blood in the absence of chemical reaction ("inert" transfer) only at high values of $P_{O_2,\infty}$. At low oxygen pressures the measured transfer rates are more than three times the theoretical inert transfer rates for the same driving force. The inert curve in Fig. 5 was calculated from equation (10) using the measured viscosity of the blood sample, the reported solubility of oxygen in blood, and the calculated effective diffusivity described above.

Carbon Dioxide Experiments

The results of the carbon dioxide extraction experiments with water are shown in Fig. 6. The data represent transfer rates measured before and after use of the membrane in a blood experiment. The theoretical line represents the case of inert transfer. It is reasonable to expect this behavior to be approached, since the kinetics of the reaction between H_2CO_3 and CO_2 are known to be slow. The data, indeed, fall near this line, especially at high values of ω. At low ω the longer residence times in the boundary layer can result in significant reaction, and natural convection becomes important. Both effects increase the transfer rate over that predicted from

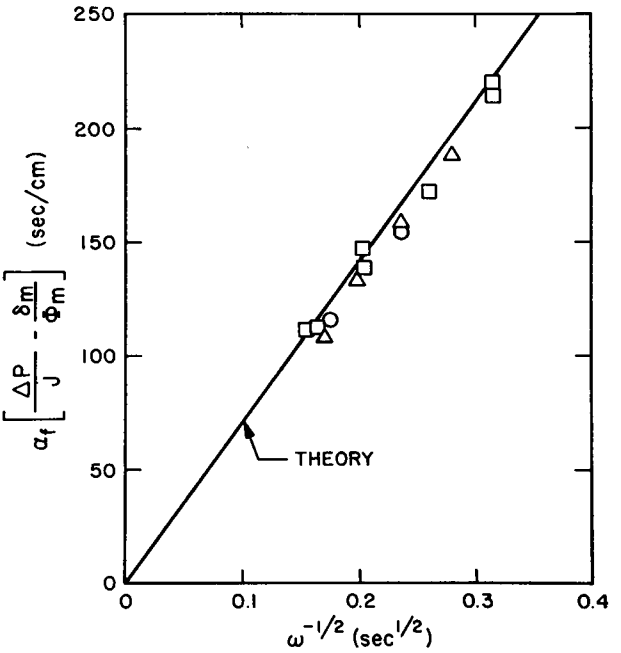

FIGURE 4 A comparison of the experimental data for oxygen desorption from water with the theoretical curve. Different symbols correspond to different membranes, and include data taken before and after use of the membrane in an experiment with freshly drawn blood. The values of $P_{O_2,\infty}$ range from 100–500 mm Hg.

theory. The data in Fig. 6 again show no change in membrane permeability as a result of exposure of the membrane to blood.

The experimental results for carbon dioxide extraction from blood with simultaneous oxygen desorption are presented in Fig. 7. The transfer rate calculated for the case of inert blood, using the measured viscosity of the blood, the reported solubility of carbon dioxide in blood, and an effective diffusivity obtained by correcting the effective diffusivity of oxygen in saturated blood, is also shown in Fig. 7. The measured transfer rates are greater than the inert model would predict, as in the case of oxygen transfer at low oxygen tension.

DISCUSSION

The data for oxygen and carbon dioxide transfer in blood show a marked enhancement of the transfer rate, over the rate predicted by equation (10) for the transfer of an inert material. It is therefore necessary to compare the data with solutions to more complicated forms of equation (6).

TABLE III

DATA FROM THE DEOXYGENATION EXPERIMENTS WITH CITRATED, FRESHLY DRAWN BLOOD AT 37.5°C

Blood sample	$P_{O_2,\infty}$	P_{O2m}*	pH	$P_{CO_2,\infty}$	ω (sec^{-1})	J_{O_2}	J_{adj}‡	J_{adj}/J_{inert}
	mm Hg	*mm Hg*		*mm Hg*		*cc(STP)/ cm²sec*		
I	79	9.0	7.4	25	19.5	25.0×10^{-6}	25.0×10^{-6}	3.53
	75	8.0			19.5	22.3×10^{-6}	22.3×10^{-6}	3.32
II	85	7.2	7.4	29	11.6	20.1×10^{-6}	20.1×10^{-6}	3.39
	77	8.2			19.2	22.9×10^{-6}	22.9×10^{-6}	3.31
	72	8.4			25.4	23.3×10^{-6}	23.3×10^{-6}	3.18
	68	9.3			35.3	25.9×10^{-6}	25.9×10^{-6}	3.19
III	290	12.5	7.2	—	11.5	34.9×10^{-6}	31.4×10^{-6}	1.57
	235	15.1			18.5	42.0×10^{-6}	37.7×10^{-6}	1.84
	187	17.5			26.8	48.5×10^{-6}	43.2×10^{-6}	2.22
	135	12.6			18.8	35.0×10^{-6}	31.1×10^{-6}	2.61
IV	405	16.6	7.25	32	18.5	46.2×10^{-6}	44.9×10^{-6}	1.27
	335	14.6			18.5	40.6×10^{-6}	39.1×10^{-6}	1.34
V	37.5	4.2	7.2	59	12.3	11.6×10^{-6}	12.2×10^{-6}	4.54
	37.5	5.0			19.9	13.9×10^{-6}	14.6×10^{-6}	4.31
	37.5	3.7			19.9	10.3×10^{-6}	10.8×10^{-6}	3.19
	37.5	3.6			19.9	9.9×10^{-6}	10.4×10^{-6}	3.07

* Calculated from J_{O_2} using the membrane permeability.

‡ The data were adjusted to the "standard" conditions listed in Table II (pH = 7.4) using the results of a parametric study on the local equilibrium model.

Oxygen Results

An interesting feature of the oxygen data shown in Fig. 5 is the approximately linear relationship exhibited by the shaded data points. These data points represent measurements taken at similar values of $P_{O_2,\infty}$ in a pressure range just above the steep portion of the blood-oxygen equilibrium curve. This linear behavior indicates the absence of a net chemical reaction term, as expected, but also suggests that local chemical equilibrium is approached in the system. If the system were not near local equilibrium, the fractional saturation of the blood would not keep pace with the

changes in oxygen tension through the boundary layer. The proximity to chemical equilibrium would then depend on the residence time of the blood in the boundary layer. Since the fluid velocities, and therefore the residence times, depend on the rotational speed, the transfer rate would not be expected to show a linear dependence on $\omega^{-1/2}$. When local equilibrium does exist, the proportionality between transfer

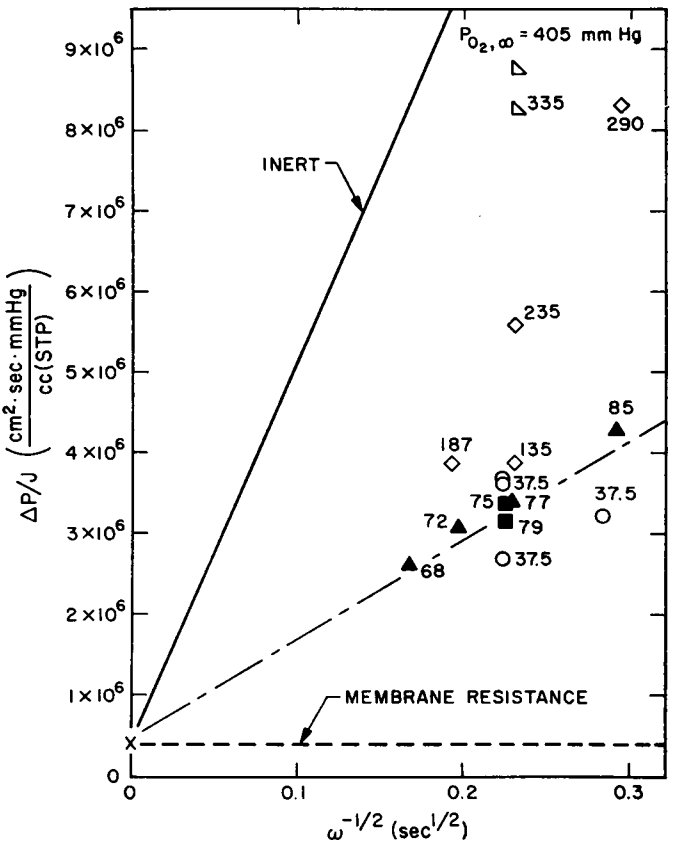

FIGURE 5 A comparison of the experimental data for the deoxygenation of citrated, freshly drawn blood with the inert theoretical curve. Different symbols correspond to different blood samples.

rate and $\omega^{-1/2}$ will hold only for a fixed set of boundary conditions. Since the shaded data points correspond to approximately the same boundary conditions, the linearity with $\omega^{-1/2}$ suggests that local chemical equilibrium is approached within the boundary layer.

Under the conditions of local chemical equilibrium the last term on the right in equation (6) vanishes. It remains, then, to specify the form of the diffusional flux $(\mathbf{J}_T)_i$. The simplest approach is to use the inert effective diffusivity, as calculated

above. The equation describing this "local equilibrium" model is then:

$$\frac{D}{Dt}(\alpha_i P_i + N_i^*) = D_{i,B}\alpha_i \nabla^2 P_i \tag{11}$$

or, for steady-state oxygen transfer in the rotating disk system:

$$v_y\left[\alpha_{O_2} + 1.34C_{Hb}\left(\frac{df}{dP_{O_2}}\right)\right]\frac{dP_{O_2}}{dy} = \alpha_{O_2}D_{O_2,B}\frac{d^2P_{O_2}}{dy^2} \tag{12}$$

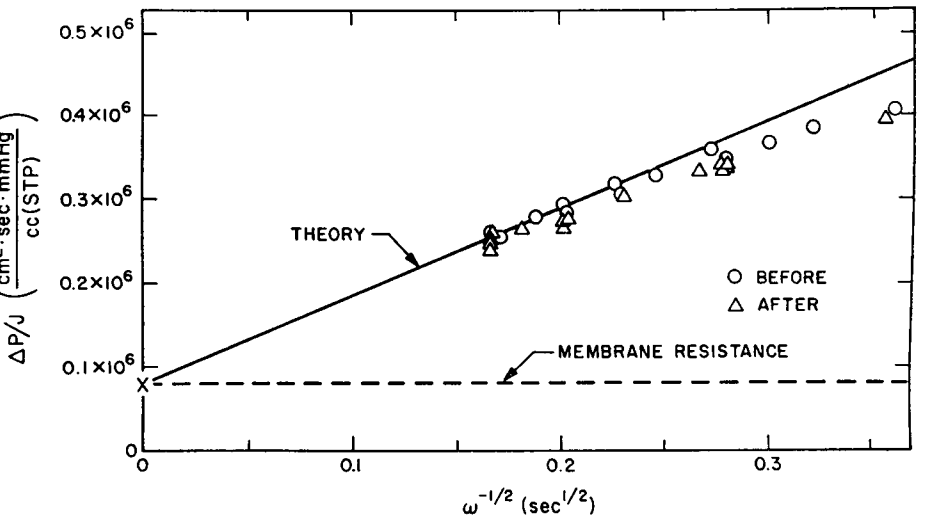

FIGURE 6 A comparison of the transfer rate data for CO_2 extraction from water, taken before and after exposure of the membrane to freshly drawn citrated blood, with the inert theoretical curve [$D_{CO_2,H_2O} = 2.82 \times 10^{-5}$ cm²/sec, $\alpha_{CO_2,H_2O} = 7.37 \times 10^{-4}$ cc (STP)/cm³ mm Hg].

For oxygen tensions corresponding to the steep region of the oxygen-oxyhemoglobin equilibrium curve, the term $1.34\ C_{Hb}(df/dP_{O_2})$ is large compared with α_{O_2}. The result, equivalent to an increased velocity, is that high concentrations of oxygen are brought close to the membrane surface, augmenting the transfer rate. This effect is shown in Fig. 8 where concentration profiles are presented for equal transfer rates. The concentrations were obtained by numerically solving the inert and local equilibrium models using the Adair constants of Roughton (26) to obtain $f(P_{O_2})$. The $P_{O_2,\infty}$ required in the local equilibrium case is a fraction of that required in the inert case, and the compression of the boundary layer is clear. This effect tapers off at higher values of $P_{O_2,\infty}$ for two reasons; the part of the boundary layer in which the oxygen-oxyhemoglobin equilibrium is active becomes a smaller fraction of the total thickness, and this region moves towards the surface of the disk. Since the

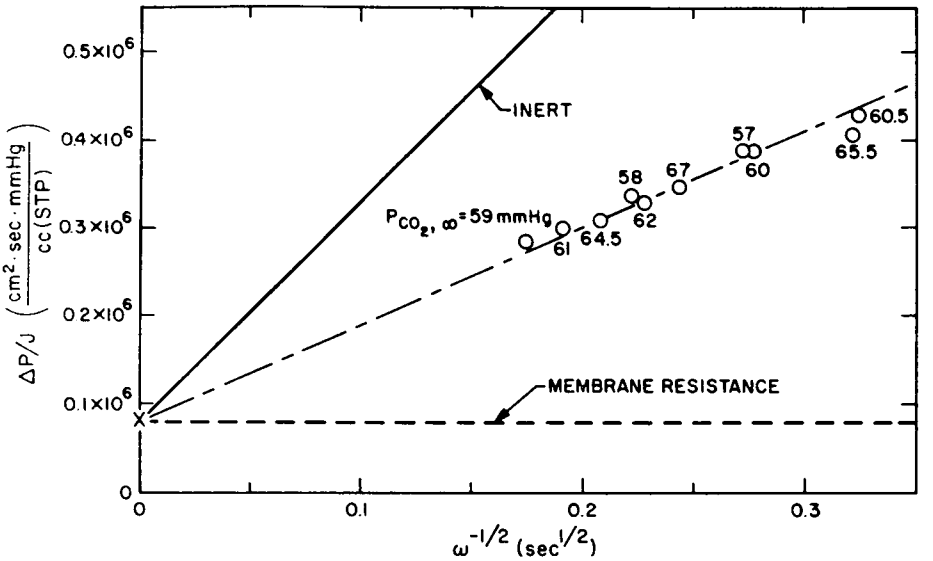

FIGURE 7 A comparison of the transfer rate data for CO_2 extraction from freshly drawn, citrated blood (P_{O_2} = 40 mm Hg, pH = 7.22, ν = 0.026 cm²/sec) with the inert theoretical curve [$D_{CO_2,B}$ = 1.3 × 10^{-5} cm²/sec, $\alpha_{CO_2,B}$ = 6.3 × 10^{-4} cc (STP)/cm³ mm Hg].

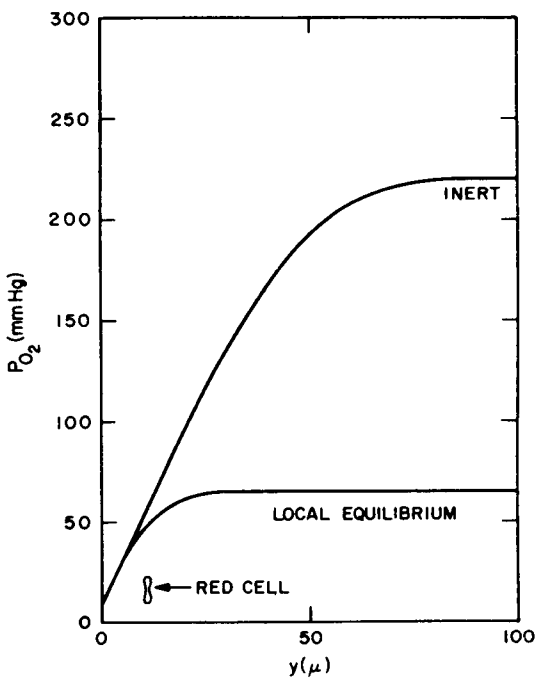

FIGURE 8 Deoxygenation concentration profiles at low P_{O_2} predicted by the inert and local equilibrium models for the same transfer rate.

velocity varies with the square of the distance from the disk, the smaller velocity tends to offset the chemical enhancement. Concentration profiles at higher $P_{O_2,\infty}$ are shown in Fig. 9, and the difference between the equilibrium and inert cases is clearly reduced.

A more complicated form of equation (6) results when facilitated diffusion is taken into account along with the local equilibrium assumption. The convective dif-

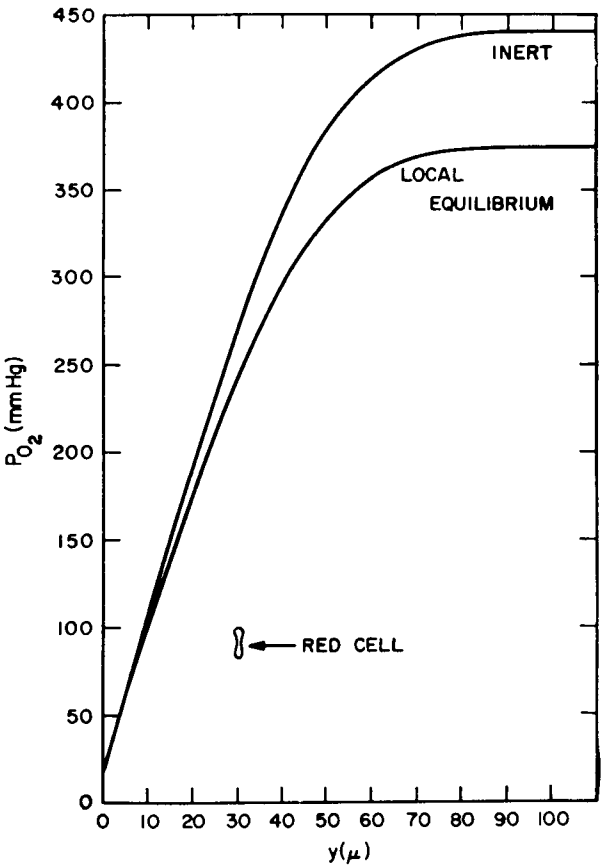

FIGURE 9 Deoxygenation concentration profiles at high P_{O_2} predicted by the inert and local equilibrium models for the same transfer rate.

fusion equation for this "facilitated local equilibrium" model is:

$$\frac{D}{Dt}(\alpha_i P_i + N_i^*) = \alpha_i \nabla \cdot (D_{i,B}^* \nabla P_i) \tag{13}$$

where $D_{i,B}^*$ is the facilitated effective diffusivity obtained from the heterogeneous media theory. For oxygen transfer, this effective diffusivity is calculated using the

following equation for the diffusivity in the red cell:

$$D^*_{O_2,RC} = D_{O_2,RC} + D_{Hb,RC}\left[\frac{1.34C_{Hb}}{\alpha_{O_2}}\right]\left(\frac{df}{dP_{O_2}}\right) \tag{14}$$

The derivation is discussed by Keller and Friedlander (12). Values of $D^*_{O_2,B}$ based on $D^*_{O_2,RC}$ calculated from this equation are given in Table IV. The hemoglobin diffusivity at red cell concentrations was obtained from Moll (21). For oxygen

TABLE IV

THE EFFECTIVE DIFFUSIVITY OF O_2 IN BLOOD AT STANDARD CONDITIONS (TABLE II), CALCULATED USING THE FACILITATED LOCAL EQUILIBRIUM MODEL, WITH $D_{Hb,RC} = 0.55 \times 10^{-7}$ cm²/sec, $D_{O_2,RC} = 1.0 \times 10^{-5}$ cm²/sec, $D_{O_2,P} = 1.57 \times 10^{-5}$ cm²/sec, and $\alpha_{O_2} = 3.0 \times 10^{-5}$ cc(STP)/cm³mm Hg

P_{O_2}	$D^*_{O_2,B}$
mm Hg	*cm²/sec*
5	1.45×10^{-5}
10	1.54 "
15	1.63 "
20	1.69 "
25	1.68 "
30	1.64 "
40	1.51 "
50	1.43 "
60	1.38 "
70	1.36 "
80	1.34 "
90	1.33 "
100	1.33 "

transfer in the rotating disk system, equation (13) becomes:

$$v_y\left[\alpha_{O_2} + 1.34C_{Hb}\left(\frac{df}{dP_{O_2}}\right)\right]\left(\frac{dP_{O_2}}{dy}\right) = \alpha_{O_2}\frac{d}{dy}\left[D^*_{O_2,B}\frac{dP_{O_2}}{dy}\right] \tag{15}$$

The measured deoxygenation rates of blood, adjusted to standard conditions, are compared with numerical solutions for these models in Fig. 10. The experimental data are best fitted by the facilitated local equilibrium model. The effect of facilitated diffusion in blood is small, however, because of the low diffusivity of the hemoglobin molecules. The local equilibrium model, although somewhat conservative, is simpler to use and represents an adequate design theory. It should be noted that good agreement with theory was obtained without taking into account carbon dioxide gradients in the boundary layer.

The assumption of local chemical equilibrium was checked by using reported equilibration rates of red cells to estimate the time required to approach equilibrium following a perturbation. Knowing the local fluid velocity, this equilibration time can then be converted into the distance traveled by the cell during the equilibration. Calculations of this type for the deoxygenation experiments (27) show that the reequilibration lengths are less than a few tenths of a micron near the surface of the disk, increasing to about 2μ at the edge of the concentration boundary layer. The assumption of local equilibrium for this system is therefore a reasonable one.

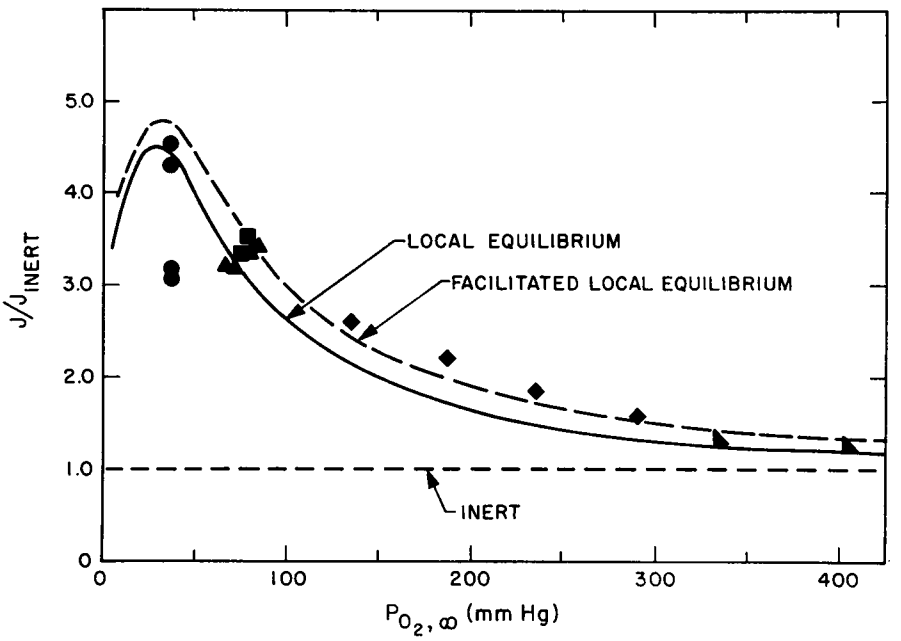

FIGURE 10 A comparison of the measured deoxygenation transfer rates in freshly drawn, citrated blood (corrected to standard conditions) with the mathematical models described in the text.

A check on the values used for the physical properties involved in the various models was made by measuring the oxygen transfer rates in a free hemoglobin solution, since it has been established that the facilitated local equilibrium model describes the behavior of this system. A hemoglobin solution was prepared from freshly drawn blood, using the procedure described by Keller and Friedlander (12), and deoxygenation transfer rate measurements were made with the rotating disk apparatus. The measured physical properties of the hemoglobin solution, and the published properties adjusted to the experimental conditions, are given in Table V. The numerical solutions for both the facilitated local equilibrium model and the local equilibrium model are shown in Fig. 11, along with the experimental data. The data fall somewhat below the facilitated local equilibrium curve, indicating some

error in the values used for the physical constants. The data do favor the facilitated local equilibrium curve, however, so the errors introduced during the calculation of the physical constants are not so large as to make the mechanisms indistinguishable.

TABLE V

MEASURED AND CALCULATED PROPERTIES USED TO DESCRIBE THE DEOXYGENATION EXPERIMENT WITH HEMOGLOBIN SOLUTION

I. Measured properties:

pH	= 7.23
P_{CO_2}	$\cong 0$
ν	= 0.015 cm²/sec
C_{Hb}	= 0.087 g/cm³
T	= 37.5°C

II. Calculated properties:

$D_{O_2,Hb}$	= 2.0×10^{-6} (cm²/sec)	(6)
$\alpha_{O_2,Hb}$	= 2.7×10^{-5} [cc(STP)/cm³mm Hg]	(6)
F_{pH}	= 0.9	(23)
$D_{Hb,Hb}$	= 6.7×10^{-7} (cm²/sec)	(13)

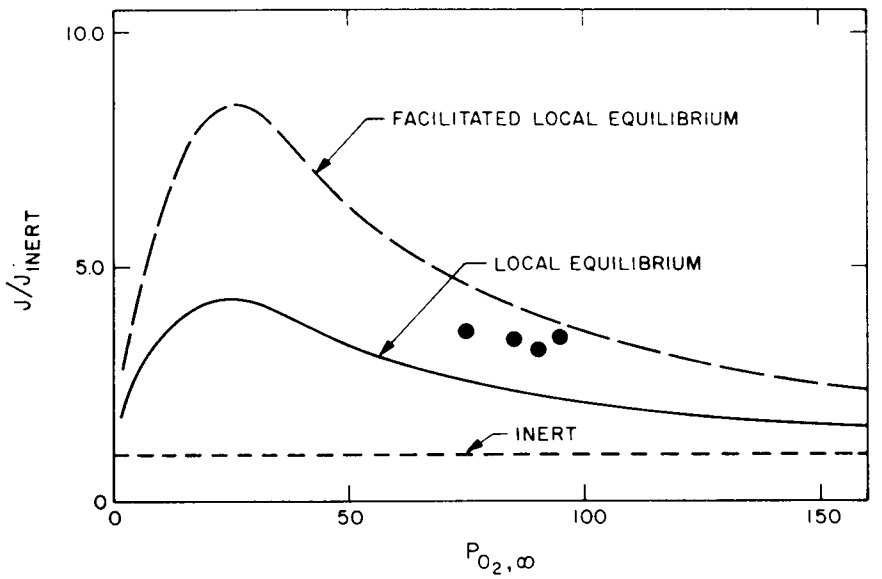

FIGURE 11 A comparison of the measured deoxygenation transfer rates in free hemoglobin solution with the mathematical models.

Carbon Dioxide Results

As in the oxygen experiments, the measured carbon dioxide transfer rates (Fig. 7) are greater than those predicted from the inert model, and an approximately linear relationship between $\Delta P/J$ and $\omega^{-1/2}$ is exhibited. As discussed above, this behavior

suggests that local chemical equilibrium is approached in the system. The data can be compared with the local equilibrium model since the carbon dioxide dissociation curve for blood, in terms of $(n_T)_{CO_2}$, is available in the literature (11). The use of the local equilibrium theory for carbon dioxide transfer cannot be justified as convincingly as in the case of oxygen transfer, since few red cell equilibration-rate measurements are available. Only the carbon dioxide uptake rate is known to have been measured (9), and that was found to be about one-third the deoxygenation rate. Since the concentration boundary layer thicknesses for carbon dioxide transfer are similar to those for oxygen transfer, the reequilibration lengths described above

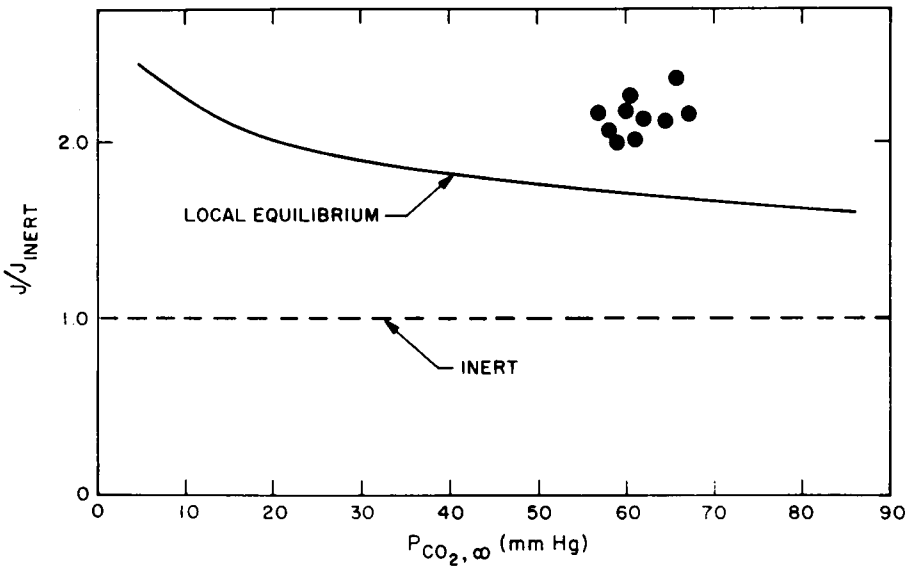

FIGURE 12 A comparison of the measured carbon dioxide removal rate from blood with the transfer rates predicted by the inert and local equilibrium models.

would have to be increased by a factor of three. This would not seriously affect the equilibrium assumption near the surface of the disk but would result in significant departure from equilibrium near the outer edge of the concentration boundary layer.

The form of equation (6) representing the local equilibrium model for carbon dioxide transfer is:

$$v_y \left[\frac{d(n_T)_{CO_2}}{dP_{CO_2}}\right] \frac{dP_{CO_2}}{dy} = \alpha_{CO_2,B} D_{CO_2,B} \left(\frac{d^2 P_{CO_2}}{dy^2}\right) \tag{16}$$

The numerical solution to equation (16) is compared with the experimental data in Fig. 12. The assumption of local equilibrium clearly does not account for all of the

measured transfer rate. A possible explanation for the high transfer rate of carbon dioxide in blood is that the diffusivity is larger than the value calculated from heterogeneous media theory because of a facilitation effect produced by the simultaneous diffusion of bicarbonate ion.

If the measured carbon dioxide removal rate is compared with the oxygen uptake rate obtained by numerically solving the local equilibrium model (27), it is found that the carbon dioxide transfer rate is 1.2–2.0 times the oxygen transfer rate, depending on the boundary conditions. If an artificial lung were to duplicate the function of the natural lung, it would have to remove enough carbon dioxide to lower the P_{CO_2} from 46 mm Hg to 40 mm Hg, and simultaneously add enough oxygen to raise the P_{O_2} from 37 mm Hg to 100 mm Hg. To do this, the transfer rate of carbon dioxide must be about 0.77 times that of oxygen. The observed carbon dioxide transfer rate is thus about 1.5–2.6 times the rate necessary to balance the oxygen transfer, and if uncorrected would lead to an excessive loss of carbon dioxide from blood circulated through a silicone-rubber membrane lung.

CONCLUSIONS

The exchange rate of an inert gas such as krypton with blood in a rotating disk boundary layer flow can be predicted from theory using Newtonian fluid hydrodynamics and effective diffusivities calculated from the theory for conduction in a heterogeneous medium. The permeabilities of silicone rubber membranes forming the surface of the disk were unchanged by exposure for several hours to fresh blood; exposure to blood previously used in a nonmembrane artificial lung resulted in a fivefold increase in membrane resistance over a period of about 1 hr because of deposition of material on the surface of the membrane. The transfer rate of oxygen in blood at low oxygen pressure is several times greater than the corresponding transfer rate of inert gas. This effect is described somewhat conservatively over a wide range of pressures by a local equilibrium model. The effect of facilitated diffusion on the transfer rate of oxygen through blood is small due to the low diffusivity of the hemoglobin molecules. The carbon dioxide transfer rate in blood near venous conditions was several times greater than the corresponding transfer rate of inert gas, but the increase in transfer could not be completely accounted for by the local equilibrium model. The carbon dioxide transfer rate in a silicone-rubber membrane system at atmospheric pressure is estimated to be from 1.5 to 2.6 times that necessary to balance the oxygen transfer rate, when the system is operated to reproduce the behavior of the natural lung.

Our study shows how solutions of the equation of convective diffusion, suitably modified, can be used to accurately predict rates of exchange of oxygen or an inert material with flowing blood. These methods should hold regardless of the geometry of the exchange system provided the characteristic hydrodynamic length (boundary layer thickness or tube diameter) is much greater than the red cell dimensions. Still

needed are careful measurements of diffusion through whole blood, when convection does not play a role, to provide experimental values for the effective diffusivities calculated in our study. Such a study made with carbon dioxide would be particularly useful.

NOMENCLATURE

C_{Hb} Hemoglobin concentration (g mole/ml)
D_{if} Diffusivity of species i through fluid f (cm²/sec)
f Fractional hemoglobin saturation
F_{pH} Severinghaus pH factor
J Transfer rate [cc(STP)/cm² sec]
$P_{i,\infty}$ Partial pressure of species i at $y = \infty$ (mm Hg)
r Radial coordinate in a cylindrical system
t Time (sec)
$\mathbf{v}$ Velocity vector (cm/sec)
v_y Velocity component normal to the disk surface (cm/sec)
y Normal distance from the disk surface
z Axial coordinate in a cylindrical system
δ_m Membrane thickness
ν Kinematic viscosity (cm²/sec)
Φ_m Membrane permeability [cc(STP)/cm sec mm Hg]
ω Angular velocity (sec⁻¹)

Superscripts

* Equilibrium value

Subscripts

$_{RC}$ Red Cell
$_S$ Serum
$_P$ Plasma
$_B$ Blood
$_m$ Membrane

This investigation was supported by the National Science Foundation Grant GP 2674 and USPHS Grant 2 T0 1 ES0004-06.

Received for publication 5 June 1967.

REFERENCES

1. BUCKLES, R. G. 1966. An analysis of gas exchange in a membrane oxygenator. Ph.D. Thesis. Massachusetts Institute of Technology, Cambridge, Mass.
2. CARSLAW, H. S., and J. C. JAEGER. 1959. Conduction of heat in solids. The Oxford University Press, London, England.
3. DE GROOT, S. R., and P. MAZUR. 1962. Non-equilibrium thermodynamics. North-Holland Publishing Company, Amsterdam, The Netherlands.
4. DOBELL, A. R. C., M. MITRI, R. GALVA, E. SARKOZY, and D. R. MURPHY. 1965. *Ann. Surg.* **161**:617.
5. FRICKE, H. 1924. *Phys. Rev.* **24**:575.
6. GOLDSTICK, T. K. 1966. Diffusion of oxygen in protein solutions. Ph.D. Thesis. University of California, Berkeley, Calif.
7. HAINLINE, A., JR. 1958. Hemoglobin. Standard Methods of Clinical Chemistry. Academic Press, Inc., New York. **2**.
8. HAINLINE, A., JR. 1965. Methemoglobin. Standard Methods of Clinical Chemistry. Academic Press, Inc., New York. **5**.

9. 1964. Handbook of Physiology—Respiration. American Physiological Society, Washington, D.C. **1** and **2**.
10. HARDEWIG, A., D. F. ROCHESTER, and W. A. BRISCOE. 1960. *J. Appl. Physiol.* **15**:723.
11. JOFFE, J. and E. P. POULTON. 1920. *J. Physiol., (London)* **54**:129.
12. KELLER, K. H., and S. K. FRIEDLANDER. 1966. *J. Gen. Physiol.* **49**:663.
13. KELLER, K. H., and S. K. FRIEDLANDER. 1966. *J. Gen. Physiol.* **49**:681.
14. LANDINO, E., J. G. MCCREARY, W. A. THOMPSON, and J. E. POWERS. 1966. *A.I.Ch.E. (Am. Inst. Chem. Engrs.) J.* **12**:117.
15. LAWSON, W. H., JR. 1966. *J. Appl. Physiol.* **21**:905.
16. LEE, W. H., JR., D. KRUMHAAR, E. W. FONKALSRUD, O. A. SCHJEIDE, and J. V. MALONEY, JR. 1961. *Surgery.* **50**:29.
17. LEVICH, V. G. 1962. Physicochemical hydrodynamics. Prentice-Hall, Inc., Englewood Cliffs, N. J.
18. MARX, T. I., W. E. SNYDER, A. D. ST. JOHN, and C. E. MOELLER. 1960. *J. Appl. Physiol.* **15**:1123.
19. MERRILL, E. W., E. R. GILLILAND, G. COKELET, H. SHIN, A. BRITTEN, and R. E. WELLS. 1963. *Biophys. J.* **3**:199.
20. MERRILL, E. W., A. M. BENIS, E. R. GILLILAND, T. K. SHERWOOD, and E. W. SALZMAN. 1965. *J. Appl. Physiol.* **20**:954.
21. MOLL, W. 1966. *Respiration Physiology.* **1**:357.
22. MORGAN, J. J., and W. STUMM. 1965. *J. Am. Water Works Assoc.* **57**:107.
23. NAERAA, N., E. S. PETERSEN, and E. BOYE. 1963. *Scand. J. Clin. Lab. Invest.* **15**:141.
24. ROBB, W. L. 1965. Report No. 65-C-031. General Electric Co., Schenectady, N.Y.
25. ROUGHTON, F. J. W. 1963. *Brit. Med. Bull.* **19**:80.
26. ROUGHTON, F. J. W. 1965. The oxygen equilibrium of mammalian hemoglobin. Oxygen, Proceedings of a Symposium Sponsored by the New York Heart Association. Little-Brown and Company. Boston, Mass.
27. SPAETH, E. E. 1967. The convective diffusion of oxygen, carbon dioxide and inert gas in blood. Ph.D. Thesis. California Institute of Technology, Pasadena, Calif.
28. WEISSMAN, M., and L. MOCKROS. 1966. Proceedings of the Annual Conference on Engineering in Medicine and Biology, San Francisco, Calif. **8**:55.
29. YOSHIDA, F., and N. OSHIMA. 1966. *J. Appl. Physiol.* **21**:915.